Extreme weather events and transmission losses in arid streams

Environmental Research Letters

LETTER

Extreme weather events and transmission losses in arid streams

Adam P Schreiner-McGraw[1,2,4], Hoori Ajami[1] and Enrique R Vivoni[2,3]

[1] Department of Environmental Sciences, University of California, Riverside, CA, 92507, United States of America
[2] School of Earth and Space Exploration, Arizona State University, Tempe, AZ, 85287, United States of America
[3] School of Sustainable Engineering and the Built Environment, Arizona State University, Tempe, AZ, 85287, United States of America
[4] Author to whom any correspondence should be addressed.

E-mail: adampschreiner@gmail.com

Keywords: dryland ecohydrology, groundwater recharge, distributed hydrologic modeling, climate change, water balance

Supplementary material for this article is available online

OPEN ACCESS

RECEIVED
27 February 2019

REVISED
5 June 2019

ACCEPTED FOR PUBLICATION
12 June 2019

PUBLISHED
22 July 2019

Abstract

A limited understanding of how extreme weather events affect groundwater hinders our ability to predict climate change impacts in drylands, where channel transmission losses are often the primary recharge mechanism. In this study, we investigate how potential changes to precipitation intensity and temperature will affect the water balance of a typical first-order, arid watershed located in the Chihuahuan Desert. We utilize a process-based hydrologic model driven by stochastically-downscaled simulations from a set of climate models, emissions scenarios, and future periods. Across many simulations, the average daily storm size is the primary factor that controls transmission losses with larger precipitation amounts increasing channel infiltration while simultaneously decreasing land surface evapotranspiration. Extreme events (>25 mm d^{-1}) that account for less than 30% of the annual precipitation, contribute almost 50% of the focused recharge. As a result, climatic changes leading to larger, less frequent storms will result in higher channel transmission losses in arid regions.

1. Introduction

Groundwater is a critical environmental resource that supplies water to billions of people and has allowed a proliferation of irrigated agriculture, particularly when surface water availability is limited (Giordano 2009, Siebert *et al* 2010, Taylor *et al* 2013). Arid and semiarid regions face water scarcity for at least part of the year and this limitation makes dryland regions particularly susceptible to climatic changes that may impact recharge rates and future groundwater availability. Due to low precipitation amounts and high temperatures in dryland regions, diffuse recharge (direct infiltration of precipitation to basin floor) is limited and a large component of groundwater recharge originates as infiltration losses in ephemeral rills and streambeds (Abdulrazzak 1995, Goodrich *et al* 2004, Shanafield and Cook 2014). Channel infiltration losses are commonly used as proxies for groundwater recharge in arid regions, due to the occurrence of deep vadose zones (Wilson and Guan 2004). Previous studies investigating channel transmission losses have found that there is a delay in the establishment of a hydraulic connection between the recharge location and the aquifer (Sorman *et al* 1997), and have conceptualized channel transmission losses as occurring when upstream flow enters a channel reach and infiltrates into the sediments, often measured with streamflow differencing approaches (Goodrich *et al* 1997).

Groundwater recharge can originate from several pathways, including mountain block recharge (Mailloux *et al* 1999), mountain front recharge (Manning and Solomon 2003), diffuse recharge (Stephens 1994, Small 2005), and focused recharge via channel transmission losses (Phillips *et al* 2004). Diffuse recharge in arid or semiarid basins has generally been found to be negligible (Gee *et al* 1994, Scanlon *et al* 1999), which makes mountain systems (including alluvial fans and piedmonts) the primary location for groundwater recharge, especially within the Basin and Range region of the United States (Ajami *et al* 2012). Streamflow from mountain systems can flow through piedmont slopes toward river valleys or endorheic playas and contribute to diffuse recharge at the playa or as transmission losses during transport downstream

(Mukhopadhyay *et al* 2003, Pelletier *et al* 2005, Costa *et al* 2012, McKenna and Sala 2018). Recent work, however, has shown the importance of infiltration losses occurring concurrently with the streamflow generation process in tributary ephemeral channels (Schreiner-McGraw and Vivoni 2017, Goodrich *et al* 2018). A rough estimate suggests that channel infiltration may contribute up to 40% of all water recharged to groundwater in a semiarid region (Pool and Dickinson 2007). Additionally, ephemeral and intermittent streams make up approximately 59% of all streams in the United States (excluding Alaska), and over 81% in the semiarid Southwest (Levick *et al* 2008). Therefore, an important knowledge gap in managing dryland water resources relates to understanding processes that control infiltration losses from ephemeral channels (Phillips *et al* 2004) and how the coupled processes of streamflow and infiltration losses will respond to extreme precipitation events (Meixner *et al* 2016). Climate model projections suggest the intensity and frequency of extreme precipitation events will increase in the future. However, the link between precipitation intensity, streamflow, and transmission losses, is non-linear and poorly quantified (Dunkerley 2012, Wasko and Sharma 2017). This suggests that extreme events are an important control for transmission losses, but the ways in which climate change will affect infiltration losses remain highly uncertain to date (Crosbie *et al* 2011, Meixner *et al* 2016).

In this study, we address this knowledge gap by using a process-based hydrologic model and stochastically-downscaled climate projections to examine the mechanisms via which climate change controls infiltration losses. We focus our analysis on infiltration occurring in tributary channels where the water supply comes from adjacent hillslopes rather than upstream channel reaches. We aim to improve predictions of climate change impacts on groundwater supplies with a focus on extreme events in the arid and semiarid Basin and Range region. We consider an extreme event to be an occurrence when daily precipitation exceeds the 97th percentile of wet days, corresponding to daily precipitation amounts greater than 25 mm at the study site in the Jornada Experimental Range (JER), New Mexico. As the projected climate change impacts on precipitation in the region are relatively uncertain, we examine the primary climatic factors that affect focused recharge in a first-order watershed. This is done using stochastically generated realizations of meteorological forcings from several general circulation models (GCMs) (as suggested by Crosbie *et al* 2011) to drive a calibrated process-based hydrologic model developed to simulate hydrologic processes of an ephemeral watershed. We aim to answer two primary questions: (1) how might changes to air temperature and precipitation affect transmission losses? and (2) how do extreme precipitation events control the ephemeral channel processes of transmission losses and streamflow?

2. Methods

2.1. Study location

Model simulations were performed in a first-order watershed located on the piedmont slope of the San Andres Mountains within the JER (figure 1). The geomorphic setting consists of north-south trending mountains abutted by a complex assemblage of landforms (e.g. alluvial fan collars, interfan valleys, and fan piedmonts) where water is conveyed from the mountains to the basin floor in ephemeral channels or via the subsurface groundwater flow system (Wondzell *et al* 1996, Phillips *et al* 2004, Rachal *et al* 2012). This geologic setting, where a first-order watershed exists on a quaternary deposit with a subtle slope is common in the Basin and Range region (USGS 1974) and drylands throughout the world. On the site piedmont slope, where woody plant encroachment has occurred (Gibbens *et al* 2005), vegetation is sparse and the majority of the study watershed is covered by bare soil (66%) with shrubs and small grass patches covering 30% and 4% of the area, respectively. The current climate at the study site is classified as desert (Köppen zone BWk, Wainwright 2006) with an average annual precipitation of 257 mm yr^{-1}, with 53% of the annual amount occurring during the North American monsoon (NAM, July–September). Short bursts of high intensity precipitation are common during the NAM and can reach rainfall intensities of 100 mm h^{-1} for several minutes (Adams and Comrie 1997). The study site was selected as representative of headwater watersheds in mountainous dryland regions and due to extensive observational data that are available for model parametrization and evaluation.

Previous investigations at the site have shown that high intensity precipitation combined with large fractions of bare soil result in infiltration excess (Hortonian-style) overland flow (Schreiner-McGraw and Vivoni 2018). Hillslope runoff flows toward ephemeral channels where the majority percolates into the sandy sediments, and the rest continues downstream and exits the watershed as streamflow (Schreiner-McGraw and Vivoni 2017). Although channel transmission losses are not necessarily equivalent to recharge, prior work has not found a consistent use of this water source by vegetation in subsequent years (Schreiner-McGraw and Vivoni 2017), indicating these losses eventually recharge the groundwater system. Within the JER, which includes mountains, piedmont slope, and basin floor, there are 1737 first-order watersheds with similar slope, geology, and drainage area, equivalent to a regional density of 2.2 watersheds per km^2. As such, characterizing precipitation properties that impact channel transmission losses is of significance beyond the study watershed.

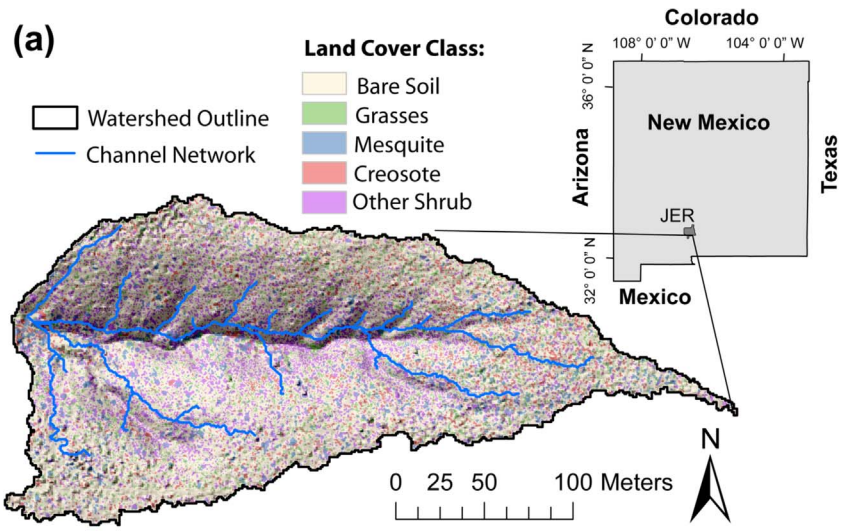

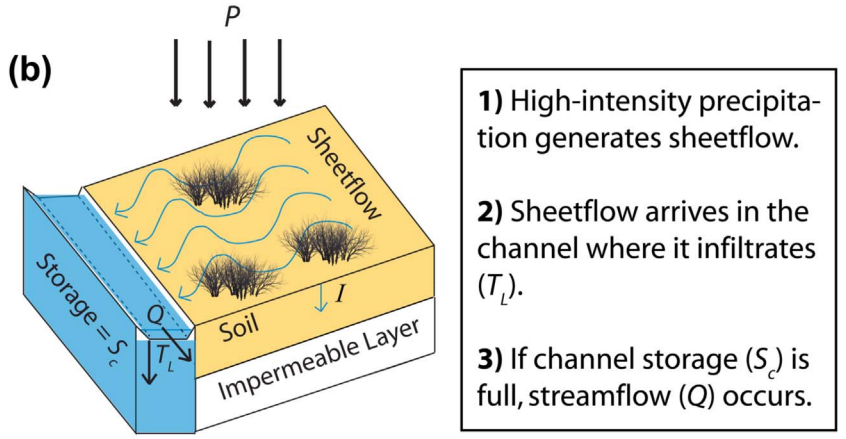

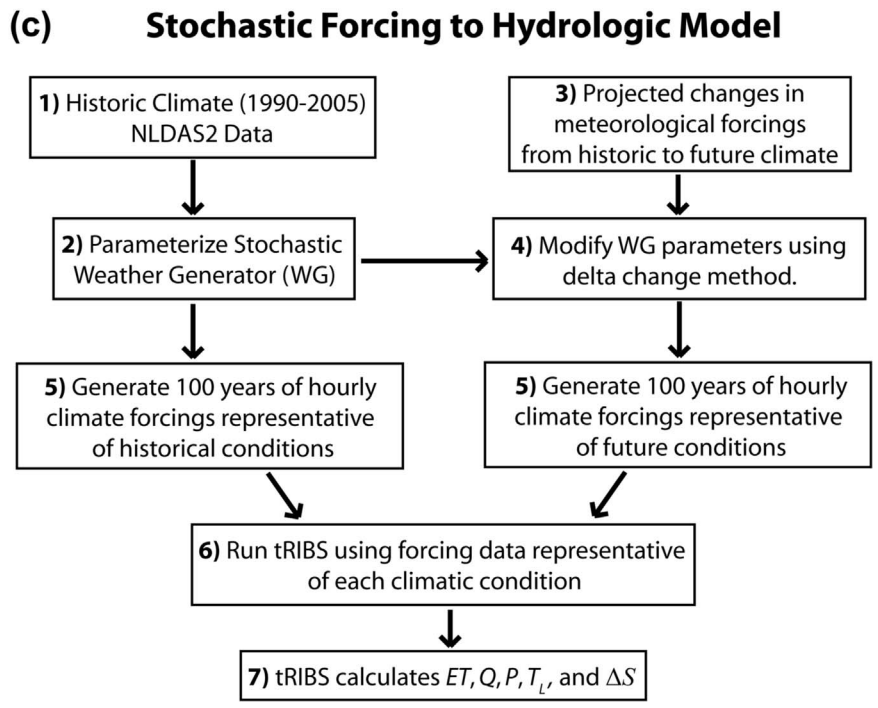

Figure 1. (a) Study site location and land cover classes used in model simulations are shown overlaying the 1 m hillshade of the study watershed generated from a UAV-derived digital elevation model. The watershed boundary and channel network are also shown. (b) Conceptual diagram of transmission losses in a first order arid streambed. (c) Flow chart demonstrating the procedure used to generate meteorological forcing data for model scenarios.

2.2. Model description

A key component facilitating channel infiltration is the difference in land surface properties, particularly soil permeability and terrain slope, between hillslopes and channels. These contrasts in slope and permeability result in concentration of runoff and recharge in the channel network (Schreiner-McGraw and Vivoni 2018). To accurately capture these differences, we make use of the TIN-based Real-time Integrated Basin Simulator (tRIBS, Ivanov *et al* 2004) parameterized at 1 m spatial resolution (model details described in supporting information is available online at stacks.iop.org/ERL/14/084002/mmedia). tRIBS supports the use of high-resolution input data (Templeton *et al* 2014) to model hillslope and channel surface processes as separate entities, which is important for simulating focused recharge. tRIBS tracks the surface water balance and infiltration fronts as they respond to a continuous input of high-resolution meteorological forcings. The model was previously modified to simulate channel transmission losses based on a conceptual model developed from a high-resolution observational study (Schreiner-McGraw and Vivoni 2017, 2018). Transmission losses are simulated for two distinct periods, (1) the 'transient period' when capillary forces act to rapidly pull water into the channel sediments as the ephemeral channel sediments initially wet and (2) the 'constant period' when sediments are saturated and infiltration occurs at a constant rate equal to the saturated hydraulic conductivity of the channel (Blasch *et al* 2006). Excess overland flow is routed downstream using the kinematic wave assumption. Given the fine temporal resolution of model simulations (1 h time step), it is possible to investigate dynamics of channel transmission losses as a function of changes in temporal patterns of precipitation. Prior efforts parameterized the model using high-resolution measurements of topography and vegetation from unmanned aerial vehicle (UAV) imagery and ancillary measurements of vegetation parameters, and evaluated the simulations against eddy covariance data, a large array of soil moisture measurements, and deep percolation estimates (Schreiner-McGraw and Vivoni 2018). A detailed description of the model setup and testing can be found in the supplemental materials (figures S1–S3). Parameters from the validated model are used here and subjected to different meteorological forcings generated to represent 16 potential future climatic forcings predicted by the GCMs that capture the climatology of the NAM region. It is important to note that as a first-order watershed, we are not discussing transmission losses from upstream flow commonly investigated in arid land streams (Costa *et al* 2012, McCallum *et al* 2014). In this study, channel transmission losses refer specifically to channel infiltration either during streamflow events or during the streamflow generation process (figure 1(b)).

2.3. Stochastic representation of future climate

We utilize a stochastic downscaling technique that applies delta change values based on the differences between the statistical properties of current and future predictions (figure 1(c), Fatichi *et al* 2011). We obtained air temperature (TA, monthly) and precipitation (P, 3 h) projections from the Coupled Model Intercomparison Project (CMIP) version 5 for three GCMs selected for their ability to represent the NAM region (Geil *et al* 2013, Verduzco *et al* 2018): (1) CNRM-CM5 (CNR), (2) CSIRO Mk3.6.0 (CSI), and (3) HadGEM2-ES (HAD). Single realizations from each model were selected for a near future period (2030–2045) and a late century period (2085–2100) whose lengths were selected to match that of a historical period (1990–2005) obtained from the North American Land Data Assimilation System (NLDAS2) reanalysis dataset (Xia *et al* 2012). Future climates are constructed for two representative concentration pathways (RCP), RCP 4.5 and RCP 8.5, using methods from Fatichi *et al* (2013) to create hourly meteorological forcings for each of the 3 GCM outputs (CNR, CSI, HAD) and their ensemble average (ENS), resulting in 16 representative future climates and 1 historical climate (HIST) scenario. Since GCM realizations were obtained at a 3 h interval, we utilized the methods of Fatichi *et al* (2013) to extend the statistical properties of precipitation to hourly resolution. As the periods of time were relatively short (15 years), we used the statistical properties of hourly forcings to generate statistically representative climates of the historical, near-future, and late-century periods as predicted by the GCMs and lasting for 100 years. Because of the inconsistency among the different GCM predictions, we focus our analyses on understanding the factors that control ephemeral channel processes rather than attempting to make an accurate prediction of the future recharge rates.

3. Results and discussion

3.1. Climate controls on water balance partitioning

Figure 2 displays the potential increases to air temperature and precipitation intensity that are outcomes of the stochastic downscaling procedure applied to historical (1990–2005, NLDAS2) and future (near-future or Mid 2030–2045 and late-century or Late 2085–2100) periods. The metrics plotted were selected to best illustrate the range of meteorological changes in the numerical experiments and to show the changes in climatic conditions that most influence transmission losses and streamflow. As expected, there is a strong warming response in all future scenarios with mean annual temperatures expected to increase by 0.3 °C–5.1 °C compared to the HIST scenario. A comparison of the annual precipitation (P) totals does not reveal such clear patterns. The mean annual P varies between scenarios with no consistent pattern in

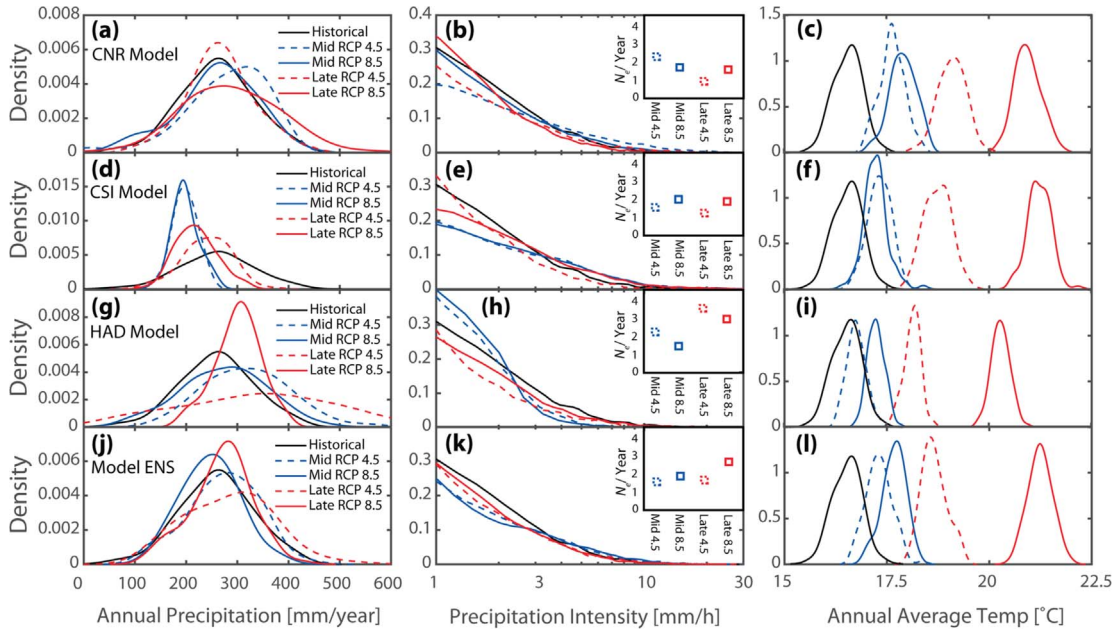

Figure 2. Comparison of meteorological conditions for historical (1990–2005) and climate change experiments (Mid: 2030–2045, Late: 2080–2100) at the study site using representative realizations from CNRM-CM5 (a)–(c), CSIRO Mk.3.6.0 (d)–(f), HadGEM2-ES (g)–(i), and their average (j)–(l). Probability density functions of annual average precipitation (a), (d), (g), (j), precipitation intensity (b), (e), (h), (k), and annual average temperature (c), (f), (i), (l). The insets in (b), (e), (h), (k) present the average number of extreme precipitation events (>25 mm d^{-1}) (N_e) per year.

time (figures 2(a), (d), (g), (j)), ranging from 182 to 346 mm yr^{-1}, with an average of 260 mm yr^{-1}. In addition, annual precipitation patterns range from highly variable (e.g. HAD late-century, RCP 4.5) to constant annual precipitation among simulation years (e.g. CSI near-future RCP 4.5 and 8.5). While the average storm properties are expected to change (Arriaga-Ramírez and Cavazos 2010), a consistent pattern in time or RCP scenario does not emerge (figures 2(a), (d), (g), (j)). The average precipitation intensity (excluding periods with no precipitation) ranges from 1.1 to 3.8 mm h^{-1} and the frequency of extreme precipitation events (>25 mm d^{-1}) ranges on average from 0.9 to 3.7 events yr^{-1}. Although this variability in predicted storm patterns reflects the uncertainty in predicting future precipitation amounts, it represents a range of plausible changes for this region that can be used to understand the climate controls on ephemeral channel processes.

Watershed responses to meteorological variations imposed by the scenarios were first investigated using the annual average climate conditions. Results indicate no significant changes in the mean annual evapotranspiration (ET), streamflow (Q), or transmission losses (T_L) due to an increase in temperature (p-values of 0.18, 0.17, and 0.28). This is contrary to recent work finding that increased temperatures result in decreased streamflow, particularly in humid regions (Udall and Overpeck 2017, Wasko and Sharma 2017). This discrepancy is likely due to the extreme water limitation at this study site (aridity index of 10) such that water availability is the primary controlling factor. In contrast to temperature increases, a change in the average annual precipitation does affect the water balance. Figures 3(a)–(c) illustrate the relations between the average annual precipitation and average annual channel T_L, ET, and Q where solid lines represent statistically significant relations ($p < 0.05$). The fact that in a water-limited environment, increases in annual P increase annual T_L and ET is not surprising (Scott *et al* 2004). However, no significant relations between annual precipitation and the ratios of partitioning precipitation into T_L/P, Q/P, and ET/P were found. Figures 3(d)–(f) show the relations between the average size of daily precipitation for wet days (S_p) and the long-term average water budget partitioning. The model allows for higher infiltration rates at the onset of flow when the streambed is dry (Blasch *et al* 2006), which could shift the balance so that frequent, small precipitation events produce the most recharge. Despite this, larger, less frequent precipitation events result in lower ratios of ET/P and higher ratios of both Q/P and T_L/P.

These results suggest that, due to the high atmospheric demand for water and the in-phase nature of maximum annual temperature and precipitation in the region, once water infiltrates into hillslope soils it evaporates sufficiently quickly that it cannot become diffuse recharge or subsurface flow supplementing streamflow. A reduction in the ratio of ET/P caused by higher intensity precipitation should affect the net ecosystem exchange and reduce the carbon uptake by the ecosystem (Biederman *et al* 2018). Higher intensity storms reduce the fraction of precipitation that

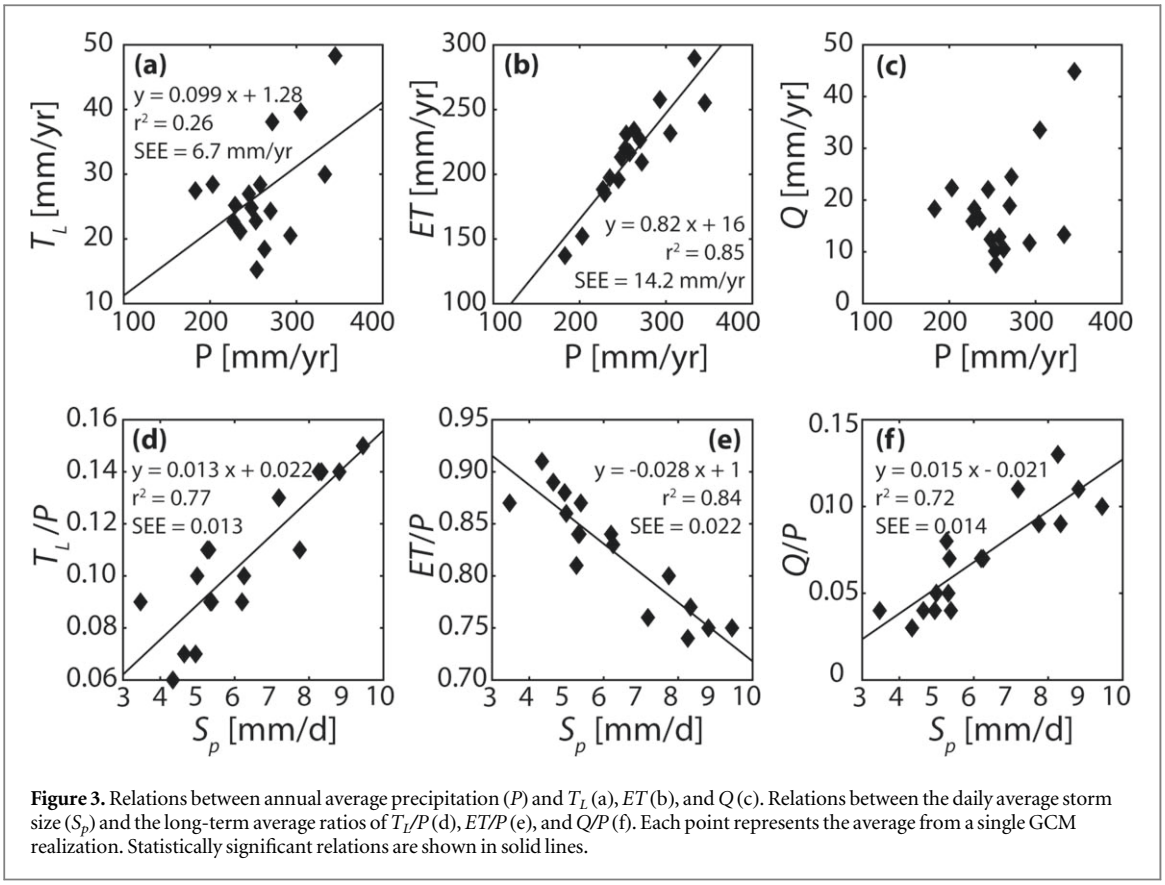

Figure 3. Relations between annual average precipitation (P) and T_L (a), ET (b), and Q (c). Relations between the daily average storm size (S_p) and the long-term average ratios of T_L/P (d), ET/P (e), and Q/P (f). Each point represents the average from a single GCM realization. Statistically significant relations are shown in solid lines.

infiltrates into the soil, affecting plant available water (PAW), and may lead to vegetation state changes. Recent research has shown that in the Basin and Range region rangeland systems where woody plant encroachment is common, shrubs perform better than grasses under water stress (Gherardi and Sala 2015, Pierce *et al* 2018). The increased streamflow and channel transmission losses ($Q + T_L$) caused by larger storm events would lower PAW and potentially favor woody plants over grasses. In contrast to the mean storm event size, the average air temperature does not appear to significantly impact PAW. In summary, the partitioning of precipitation on hillslopes between infiltration and overland flow that becomes Q or T_L depends on the storm event size, which is the primary control on water budget partitioning in this system.

3.2. Extreme precipitation events controls on transmission losses and streamflow

After examining long-term conditions, the calibrated process-based hydrologic model is used to determine how event scale precipitation interacts with the soil properties to control channel transmission processes. For each representative scenario, we built relations at an event scale between transmission losses and several precipitation properties: daily storm event size (S_p), storm duration (T_p), average precipitation rate (α), and weighted hourly precipitation intensity (INT). We define α as the average precipitation intensity during a storm and INT with the following equation from Tashie *et al* (2016):

$$INT = \frac{\sum (HI)^2}{S_p}, \quad (1)$$

where HI is the hourly precipitation intensity. Figures 4(a), (b) illustrates the slope and r^2 values for each relation between transmission losses and the precipitation properties, where the symbols represent the values from individual simulations and diamonds are average values for all realizations. Factors that most control the transmission losses are the average daily storm event size and the average precipitation rate (slope $= 0.1$ and 0.3; $r^2 = 0.31$ and 0.32, respectively; $p \ll 0.05$). These findings highlight the importance of individual storm events in controlling infiltration losses during streamflow generation and suggest that understanding the impact of high intensity, extreme precipitation is important for groundwater management.

Consistent with observations, extreme precipitation events are predicted to become more common in most of the future climate scenarios (figure 2) (Luong *et al* 2017). We divided the precipitation events into six classes displayed in figure 4(c), which illustrates the contribution of each precipitation size class to the total precipitation and channel transmission losses. This shows that while 20% of the total precipitation is contributed by small storms (0–5 mm), small storms only account for 8% of the total channel infiltration. Extreme events (>25 mm), however, constitute 29% of the total precipitation, but contribute 46% of the

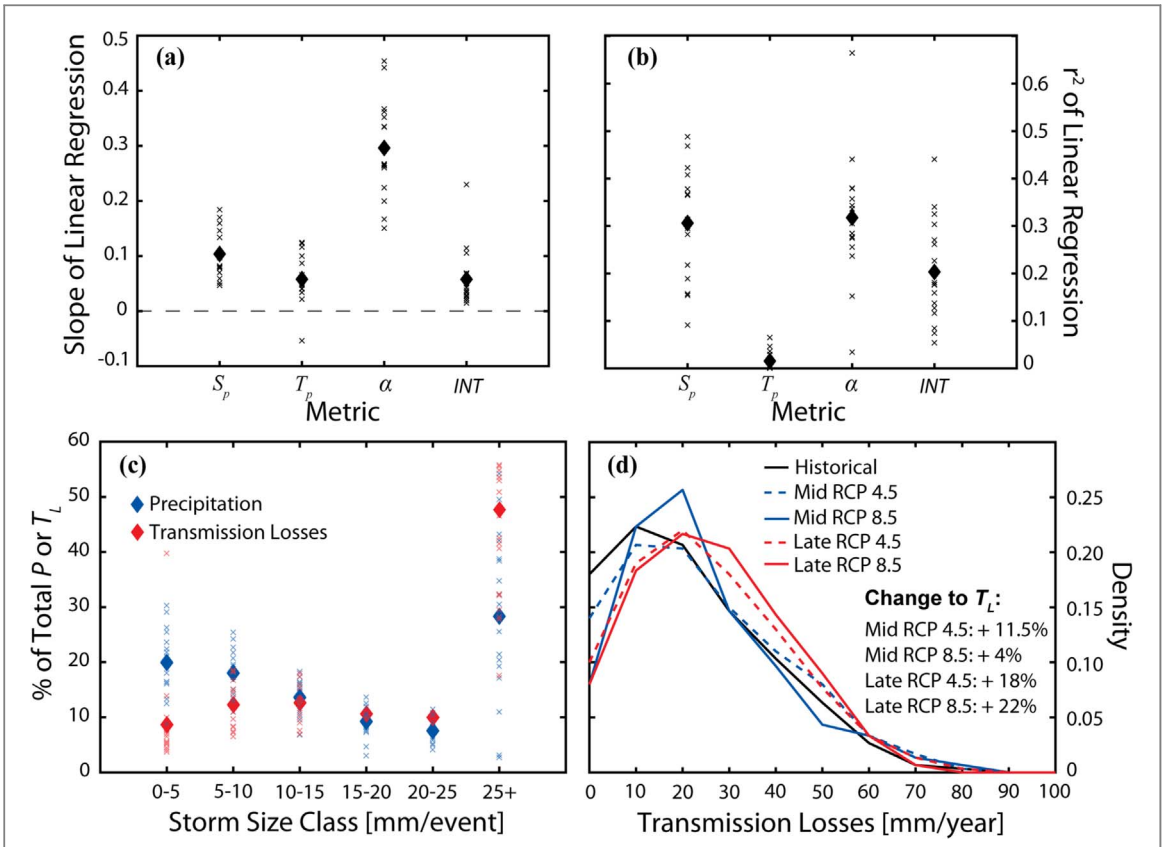

Figure 4. (a) Slope and (b) r^2 values for the relations between transmission losses attributed to a precipitation event and precipitation metrics. Each climate realization is shown as an *x* and the mean value is displayed as a large diamond. (c) Percentage of total precipitation (blue) and transmission losses (red) contributed by each storm size class. (d) Probability density functions of annual transmission losses for the average (ENS) scenario and the historical (HIST) simulation. The average increase in T_L from each climate realization is shown.

channel infiltration (figure 4(c)). Calculated ratios of transmission losses to precipitation (T_L/P) for each precipitation class show that extreme precipitation events (>25 mm) contribute 22% of their amount to channel infiltration as compared to only 5% of precipitation contributing to transmission losses for any precipitation event smaller than 25 mm. This contribution to transmission losses following extreme precipitation events suggests that a shift to more extreme precipitation events will dramatically increase T_L/P. This increase is illustrated in figure 4(d) which presents probability density functions of the annual transmission losses for the historical and average (ENS) future scenarios. Near future (2030–2045) scenarios predict an increase of 4% to 11.5% in annual transmission losses, while the late century (2085–2100) scenarios predict an increase of 18%–22% to transmission losses due to more extreme precipitation events.

While extreme events are important for producing transmission losses, they are even more important in producing streamflow. Figure 5 illustrates the effect of the average number of precipitation events per year (N_e) for different storm sizes on the partitioning of overland flow into transmission losses and streamflow, T_L/Q. In climate realizations with more frequent small precipitation events (<10 mm, figures 5(a), (b)), T_L/Q increases with N_e ($p < 0.0001$, $r^2 > 0.54$). In contrast, climate realizations with more extreme precipitation events (>25 mm, figure 5(f)) have ephemeral channels that produce larger quantities of streamflow and reduce T_L/Q with N_e ($p < 0.0001$ and $r^2 = 0.448$). For intermediate sized precipitation events, no clear patterns are found in the partitioning between transmission losses and streamflow. This behavior is a result of rapid infiltration of overland flow into channels that occurs until the channel storage capacity is filled and streamflow can then begin (Schreiner-McGraw and Vivoni 2017). As a result, streamflow is more sensitive to extreme events than transmission losses, suggesting additional impacts such as increases in erosion in first-order watersheds (Whipple and Tucker 1999). Changes to erosion in the future may also impact transmission losses by impacting channel geometry and sediment properties. For a discussion of the effect of changes in channel hydraulic conductivity, the reader is referred to Schreiner-McGraw and Vivoni (2018). Due to constant channel geometry in our simulations (and therefore constant channel storage capacity), ephemeral streamflow is more sensitive to extreme precipitation events than transmission losses.

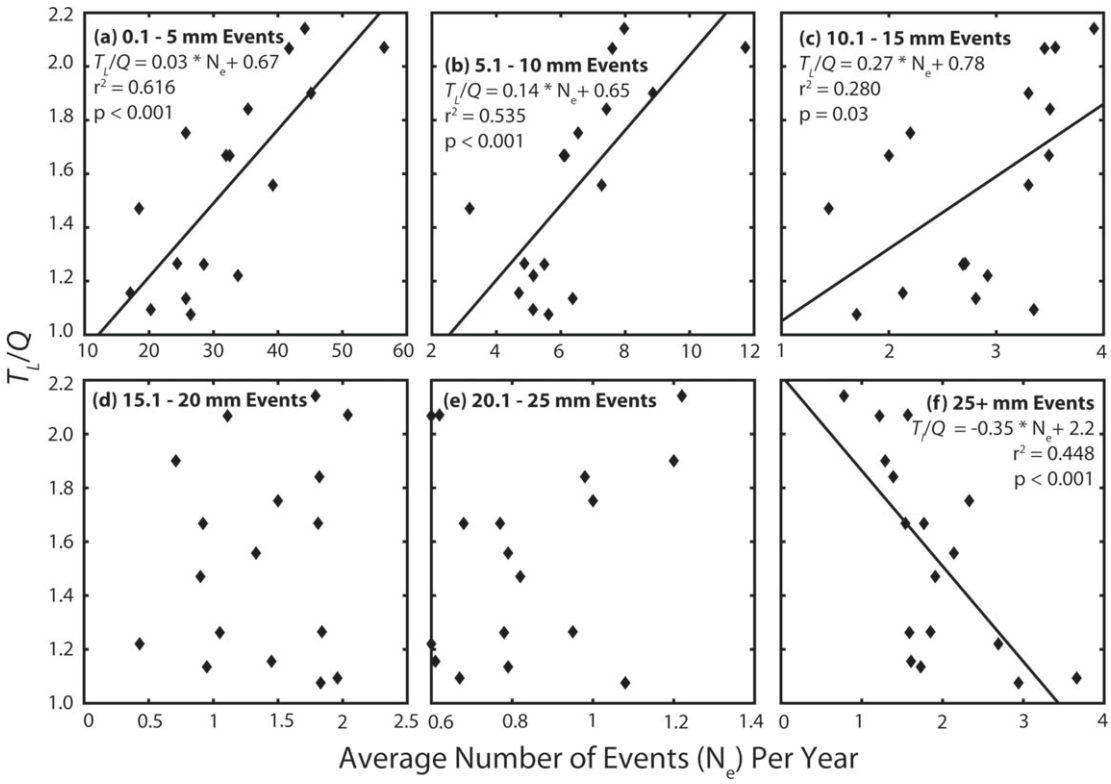

Figure 5. Relations between the average number of precipitation events of each size class per year and T_L/Q. Statistically significant relations are shown as solid lines.

4. Concluding remarks

We studied the impacts of climate change on the response of an ephemeral watershed using a process-based hydrologic model and stochastic downscaling of climate change projections. We found that increases in air temperature do not alter the water balance of the study watershed and attributed this to the high aridity index. The total annual precipitation exerts a strong control on *ET* and a weak control on transmission losses, but precipitation totals do not affect the water balance partitioning. We identified the primary climatic factor controlling the water balance partitioning ratios to be the average size of precipitation events. Small, but frequent, storms allow more hillslope infiltration which increases the soil water available for *ET*; whereas large, infrequent storms create more overland flow that becomes streamflow and transmission losses when it reaches the channel network. This result suggests that if the frequency of extreme precipitation events increases in the future, both transmission losses and streamflow will increase within the piedmont slopes of the Basin and Range province.

Small, frequent precipitation events result in the vast majority of water infiltrating into the soil to become available for *ET*, and on average only 5% of event precipitation becomes transmission losses. In contrast, large, infrequent precipitation events overwhelm hillslope infiltration rates and 22% of the event precipitation percolates via channel sediments and is potentially available for groundwater recharge. More importantly, extreme events ($>25\,\mathrm{mm\,d^{-1}}$) that account for less than 30% of the total precipitation, contribute almost 50% of the total transmission losses. While extreme precipitation plays an outsized role in generating transmission losses, these events are even more important for generating streamflow as they quickly exceed channel infiltration capacities and generate significant streamflow. Climatic changes that result in larger, less frequent storms will reduce soil water availability and increase transmission losses and streamflow. These results suggest that climate change may increase recharge rates (Villeneuve *et al* 2015) in the Basin and Range region, increasing groundwater availability at the expense of PAW.

Acknowledgments

We thank John Anderson and other staff members of the USDA-ARS and Jornada LTER for field and data support. Funding provided by the Jornada LTER (DEB-1235828), Army Research Office (56059-EV-PCS), USDA multi-state W3188, UC Office of the President's Multi-Campus Research Programs and Initiatives (MR-15-328473) through UC Water, the University of California Water Security and Sustainability Research Initiative, and USDA NIFA Graduate Fellowship program (2017-67011-26069) to A S-M is acknowledged. We are grateful to R C Templeton, C A

Anderson and E R Peréz-Ruíz for their field activities. Datasets for the site are available at the Jornada Data Catalog (http://jornada.nmsu.edu/lter/data).

ORCID iDs

Adam P Schreiner-McGraw https://orcid.org/0000-0003-3424-9202
Hoori Ajami https://orcid.org/0000-0001-6883-7630
Enrique R Vivoni https://orcid.org/0000-002-2659-9459

References

Abdulrazzak M J 1995 Losses of flood water from alluvial channels *Arid Land Resour. Manage.* **9** 15–24
Adams D K and Comrie A C 1997 The North American monsoon *Bull. Am. Meteorol. Soc.* **78** 2197–213
Ajami H, Meixner T, Dominguez F, Hogan J F and Maddock T III 2012 Seasonalizing mountain system recharge in semi-arid basins: climate change impacts *Ground Water* **50** 585–97
Arriaga-Ramírez S and Cavazos T 2010 Regional trends of daily precipitation indices in northwest Mexico and southwest United States *J. Geophys. Res.* **115** D14111
Biederman J A, Scott R L, Arnone J A III, Jasoni R L, Litvak M E, Moreo M T, Papuga S A, Ponce-Campos G E, Schreiner-McGraw A P and Vivoni E R 2018 Shrubland carbon sink depends upon winter water availability in the warm deserts of North America *Agric. For. Meteorol.* **249** 407–19
Blasch K W, Ferré T P A, Hoffmann J P and Fleming J B 2006 Relative contributions of transient and steady state infiltration during ephemeral streamflow *Water Resour. Res.* **42** W08405
Costa A C, Bronstert A and de Araújo J C 2012 A channel transmission losses model for different dryland rivers *Hydrol. Earth Syst. Sci.* **16** 1111–35
Crosbie R S, Dawes W R, Charles S P, Mpelasoka F S, Aryal S, Barron O and Summerell G K 2011 Differences in future recharge estimates due to GCMs, downscaling methods and hydrological models *Geophys. Res. Lett.* **38** L11406
Dunkerley D 2012 Effects of rainfall intensity fluctuations on infiltration and runoff: rainfall simulation on dryland soils, Fowlers gap, Australia *Hydrol. Process.* **26** 2211–24
Fatichi S, Ivanov V Y and Caporali E 2011 Simulation of future climate scenarios with a weather generator *Adv. Water Res.* **34** 448–67
Fatichi S, Ivanov V Y and Caporali E 2013 Assessment of a stochastic downscaling methodology in generating an ensemble of hourly future climate time series *Clim. Dyn.* **40** 1841–61
Gee G W, Wierenga P J, Andraski B J, Young M H, Fayer M J and Rockhold M L 1994 Variations in water balance and recharge potential at three western desert sites *Soil Sci. Soc. Am. J.* **58** 63–72
Geil K L, Serra Y L and Zeng X 2013 Assessment of CMIP5 model simulations of the North American monsoon system *J. Clim.* **26** 8787–801
Gherardi L A and Sala O E 2015 Enhanced precipitation variability decreases grass- and increases shrub-productivity *Proc. Natl Acad. Sci.* **112** 12735–40
Gibbens R P, McNeely R P, Havstad K M, Beck R F and Nolen B 2005 Vegetation changes in the Jornada Basin from 1858 to 1998 *J. Arid Environ.* **61** 651–68
Giordano M 2009 Global groundwater? Issues and solutions *Annu. Rev. Environ. Resour.* **34** 153–78
Goodrich D C, Kepner W G, Levick L R and Wigington P J Jr 2018 Southwestern intermittent and ephemeral stream connectivity *J. Am. Water Resour. Assoc.* **54** 400–22
Goodrich D C, Lane L J, Shillito R M and Miller S N 1997 Linearity of basin response as a function of scale in a semiarid watershed *Water Resour. Res.* **33** 2951–65
Goodrich D C, Williams D G, Unkrich C L, Hogan J F, Scott R L, Hultine K R, Pool D, Coes A L and Miller S 2004 Comparison of methods to estimate ephemeral channel recharge, Walnut Gulch, San Pedro River Basin, Arizona *Groundwater Recharge in a Desert Environment* ed J F Hogan *et al* (Washington, DC: American Geophysical Union) pp 77–99
Ivanov V Y, Vivoni E R, Bras R L and Entekhabi D 2004 Catchment hydrologic response with a fully-distributed triangulated irregular network model *Water Resour. Res.* **40** W11102
Levick L 2008 *The Ecological and Hydrological Significance of Ephemeral and Intermittent Streams in the Arid and Semi-Arid American Southwest* EPA/600/R-08/134, ARS/233046 US Environmental Protection Agency and USDA/ARS Southwest Watershed Research Center 116p
Luong T M, Castro C L, Chang H I, Lahmers T, Adams D K and Ochoa-Moya C A 2017 The more extreme nature of North American monsoon precipitation in the southwestern United States as revealed by a historical climatology of simulated severe weather events *J. Appl. Meteorol. Climatol.* **56** 2509–29
Mailloux B J, Person M, Kelley S, Dunbar N, Cather S, Strayer L and Hudleston P 1999 Tectonic controls on the hydrogeology of the Rio Grande rift, New Mexico *Water Resour. Res.* **35** 2641–59
Manning A H and Solomon D K 2003 Using noble gases to investigate mountain-front recharge *J. Hydrol.* **275** 194–207
McCallum A M, Andersen M S, Rau G C, Larsen J R and Acworth R I 2014 River-aquifer interactions in a semiarid environment investigated using point and reach measurements *Water Resour. Res.* **50** 2815–29
McKenna O P and Sala O E 2018 Groundwater recharge in desert playas: current rates and future effects of climate change *Environ. Res. Lett.* **13** 014025
Meixner T *et al* 2016 Implications of projected climate change for groundwater recharge in the western United States *J. Hydrol.* **534** 124–38
Mukhopadhyay B, Cornelius J and Zehner W 2003 Application of kinematic wave theory for predicting flash flood hazards on coupled alluvial fan-piedmont plain landforms *Hydrol. Process.* **17** 838–68
Pelletier J D, Mayer L, Pearthree P A, House P K, Demsey K A, Klawon J E and Vincent K R 2005 An integrated approach to flood hazard assessment on alluvial fans using numerical modeling, field mapping and remote sensing *GSA Bull.* **117** 1167–80
Phillips F M, Hogan J F and Scanlon B R 2004 Introduction and overview *Groundwater Recharge in a Desert Environment* ed J F Hogan *et al* (Washington, DC: American Geophysical Union) pp 1–14
Pierce N, Archer S R, Bestelmeyer B T and James D K 2018 Grass-shrub competition in arid lands: an overlooked driver in grassland-shrubland state transitions? *Ecosystems* **21** 1–10
Pool D R and Dickinson J E 2007 'Ground-water flow model of the Sierra Vista subwatershed and Sonoran portions of the Upper San Pedro Basin, southeastern Arizona, United States, and Northern Sonora, Mexico *Prepared in Cooperation with the Upper San Pedro Partnership and Bureau of Land Management* (Reston, VA: US Department of the Interior, US Geological Survey)
Rachal D M, Monger H C, Okin G S and Peters D C 2012 Landform influences on the resistance of grasslands to shrub encroachment, Northern Chihuahuan Desert, USA *J. Maps* **8** 507–13
Scanlon B R, Langford R P and Goldsmith R S 1999 Relationship between geomorphic settings and unsaturated flow in an arid setting *Water Resour. Res.* **35** 983–99
Schreiner-McGraw A P and Vivoni E R 2017 Percolation observations in an arid piedmont watershed and linkages to historical conditions in the Chihuahuan Desert *Ecosphere* **8** e02000

Schreiner-McGraw A P and Vivoni E R 2018 On the sensitivity of hillslope runoff and channel transmission losses in arid piedmont slopes *Water Resour. Res.* **54** 4498–518

Scott R L, Edwards E A, Shuttleworth W J, Huxman T E, Watts C and Goodrich D C 2004 Interannual and seasonal variation in fluxes of water and carbon dioxide from a riparian woodland ecosystem *Agric. For. Meteorol.* **122** 65–84

Shanafield M and Cook P G 2014 Transmission losses, infiltration and groundwater recharge through ephemeral and intermittent streambeds: a review of applied methods *J. Hydrol.* **511** 518–29

Siebert S, Burke J, Faures J M, Frenken K, Hoogeveen J, Döll P and Portmann F T 2010 Groundwater use for irrigation—a global inventory *Hydrol. Earth Syst. Sci.* **14** 1863–80

Small E E 2005 Climatic controls on diffuse groundwater recharge in semiarid environments of the southwestern United States *Water Resour. Res.* **41** W04012

Sorman A U, Abdulrazzak M J and Morel-Seytoux H J 1997 Groundwater recharge estimation from ephemeral streams. Case study: wadi tablah, Saudi Arabia *Hydrol. Process.* **11** 1607–19

Stephens D B 1994 A perspective on diffuse natural recharge mechanisms in areas of low precipitation *Soil Sci. Soc. Am. J.* **58** 40–8

Tashie A M, Mirus B B and Pavelsky T M 2016 Identifying long-term empirical relationships between storm characteristics and episodic groundwater recharge *Water Resour. Res.* **51** 21–35

Taylor R G *et al* 2013 Ground water and climate change *Nat. Clim. Change* **3** 322–9

Templeton R C, Vivoni E R, Méndez-Barroso L A, Pierini N A, Anderson C A, Rango A, Laliberte A S and Scott R L 2014 High-resolution characterization of a semiarid watershed: implications on evapotranspiration estimates *J. Hydrol.* **509** 306–19

Udall B and Overpeck J 2017 The twenty-first century Colorado River hot drought and implications for the future *Water Resour. Res.* **53** 2404–18

USGS 1974 Geologic Map of the United States (Reston, VA: US Geological Survey) ((https://doi.org/10.3133/70136641))

Verduzco V S, Vivoni E R, Yépez E A, Rodríguez J C, Watts C J, Tarin T, Garatuza-Payán J, Robles-Morua A and Ivanov V Y 2018 Climate change impacts on net ecosystem productivity in a subtropical shrubland of Northwestern Mexico *J. Geophys. Res.: Biogeosci.* **123** 688–711

Villeneuve S, Cook P G, Shanafield M, Wood C and White N 2015 Groundwater recharge via infiltration through an ephemeral riverbed, central Australia *J. Arid Environ.* **117** 47–58

Wainwright J 2006 Climate and climatological variations in the Jornada Basin *Structure and Function of a Chihuahuan Desert Ecosystem* ed K M Havstad *et al* (New York, NY: Oxford University Press) pp 44–80

Wasko C and Sharma A 2017 Global assessment of flood and storm extremes with increased temperatures *Sci. Rep.* **7** 7945

Whipple K X and Tucker G E 1999 Dynamics of the stream-power river incision model: implications for height limits of mountain ranges, landscape response timescales, and research needs *J. Geophys. Res.—Solid Earth* **104** 17661–74

Wilson J L and Guan H 2004 Mountain-block hydrology and mountain-front recharge *Groundwater Recharge in a Desert Environment* ed J F Hogan *et al* (Washington, DC: American Geophysical Union) pp 113–35

Wondzell S M, Cunningham G L and Bachelet D 1996 Relationships between landforms, geomorphic processes, and plant communities on a watershed in the northern Chihuahuan Desert *Landscape Ecol.* **11** 351–62

Xia R *et al* 2012 Continental-scale water and energy flux analysis and validation for the North American Land Data Assimilation System project phase 2 (NLDAS-2): I. Intercomparison and application of model products *J. Geophys. Res.* **117** D03109